

STUDY ON FLEXURAL DUCTILITY ENHANCEMENT OF REINFORCED CONCRETE WALLS BY TRANSVERSE CONFINING STEEL

T. Nakachi¹

¹ Professor, Dept. of Architecture and Civil Engineering, Architecture Major,
Fukui University of Technology, Fukui, Japan
Email: nakachi@fukui-ut.ac.jp

ABSTRACT:

Multistory core walls installed in high-rise reinforced concrete buildings effectively reduce seismic vibration. In high-rise buildings with the core wall system, which consists of four L-shaped core walls, the axial load of the core wall is remarkably high under the action of a diagonal seismic force. In particular, the corner and the area near the corner of the L-shaped core walls are subject to high compressive stress. Reinforcing these areas is therefore considered effective for improving the deformation capacity of the core walls. On the other hand, in wall columns with a rectangular section, the edge area is subjected to high compressive and shear stress at flexural yielding; reinforcing this area is considered to be effective for improving the deformation capacity of the wall columns. This paper examines the relationship between the confinement effect or reinforcement arrangement of these areas and the deformation capacity of the reinforced concrete walls. The evaluation was based on the results of core wall lateral loading and compression tests. Based on the results of lateral loading tests of L-, T-, H-shaped core walls and wall columns, an edge confinement index was proposed. This index is composed of the confinement effect of concrete, confinement area, axial stress, and depth-to-width ratio. The relationship between the edge confinement index and limit drift angle was shown.

KEYWORDS: shear wall, core wall, deformation capacity, confining steel, axial load

1. INTRODUCTION

Reinforcing the areas of core walls that come under high compressive stress is considered to be effective for improving their deformation capacity. Previously, the authors conducted lateral loading tests of multistory L-shaped reinforced concrete core walls¹⁾. The test parameters were the concrete confinement at the corner, the amount of confining steel at the corner, and the area of concrete confinement. Based on the results of core wall lateral loading tests and compression tests on square and rectangular section columns which simulated the corner area of core walls, the deformation capacity of core walls was evaluated. The authors also studied the deformation capacity of wall columns with a rectangular section in relation to the confinement of edge area concrete. In this paper, an edge confinement index is proposed based on the results of lateral loading tests of core walls and wall columns. The relationship between the edge confinement index and limit drift angle is shown.

2. THE DEFORMATION CAPACITY OF WALL COLUMNS BY CONFINING STEEL

Previously, the authors conducted lateral loading tests of wall columns with a rectangular section and compression tests on rectangular section columns which simulated the edge area of wall columns. The test results showed the effectiveness of confinement of the edge concrete on the deformation capacity of wall columns²⁾. Furthermore, the results of compression tests were simulated with Mugeruma's equation³⁾ which shows the stress-strain relations of confined concrete, and wall columns were analyzed by fiber model analysis with Mugeruma's equation⁴⁾. The analysis results

showed that a larger amount of confining steel significantly improved the deformation capacity of the wall columns.

The authors also conducted lateral loading tests of wall columns using the parameters of depth-to-width ratio, confinement area at the edge and axial stress⁵⁾. The results of these tests showed that the limit drift angle decreases as the depth-to-width ratio and axial stress increase, and increases as the confinement area increases. Based on these results, Hiraishi et al. proposed a mechanical model for the deformation of wall columns beyond flexural yielding, and represented the drift angle when the seismic capacity of wall columns began to decrease by the following equation⁶⁾:

$$R \cong \alpha \varepsilon_{cu} / \{ (\sigma_0 / F_c) \cdot (D/b) \} \quad (2.1)$$

where R = drift angle; α = index representing height of concrete plastic zone; αb = height of concrete plastic zone; ε_{cu} = average strain at compressive end of concrete plastic zone when the seismic capacity of wall columns begins to decrease; $\sigma_0 = N/(b D)$; N = axial load; F_c = concrete compressive strength; D = depth of wall column; and b = width of wall column. In this equation, the height of the concrete plastic zone is assumed to depend on the width, not depth, of the wall column. It is also assumed that the distance from the compressive end to the neutral axis is $(\sigma_0 / F_c)D$ and that compressive ductility at the edge confined area of the wall column is constant.

3. LATERAL LOADING TEST OF CORE WALLS

Authors previously conducted lateral loading tests of core walls of which parameters were the concrete confinement at the corner, the amount of confining steel at the corner, and the area of concrete confinement¹⁾. Outline of the tests are as follows.

3.1 Test Specimens

The configuration and arrangement of reinforcing in the specimens are shown in Fig. 1. Four one-eighth-scale core wall specimens were tested. Each specimen represented the core walls of the lower three stories of a high-rise building of approximately twenty-five stories. The specimens had a shear span ratio of 2.5. The specified design concrete strength was 588 N/mm^2 . The physical properties of the concrete and reinforcement are listed in Tables 1 and 2, respectively. All of the specimens were the flexural type. Specimen L1 had no confining reinforcement. Specimen L2 was confined at the corner using square closed reinforcement. Specimens L3 and L4 were confined at the area near the corner using tie bars. Specimen L4 had twice the number of tie bars as Specimen L3. The confining bars were arranged up to a height corresponding to the second floor level (h : 615 mm).

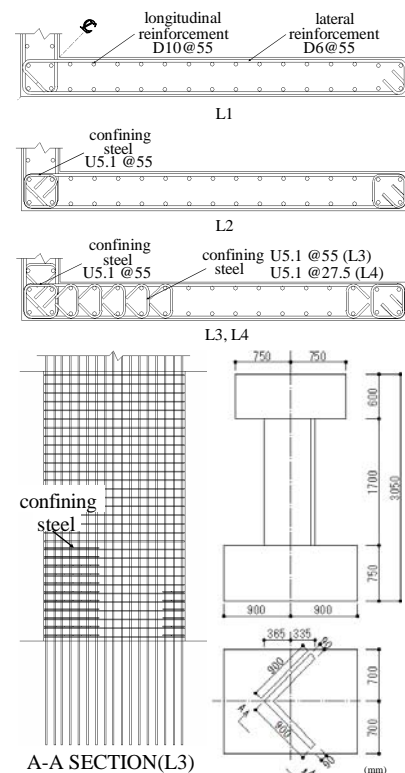


Fig. 1 Test specimens

3.2 Test Procedure

In the cyclic lateral loading tests, the specimens were subjected to forces by an actuator connected to the reaction wall. A constant axial loading force was applied by a hydraulic jack over the specimen to represent the axial stress in the stage of coupling beam yielding at the center core. The axial stress

was 60% of the concrete compressive cylinder strength at the positive loading for which the corner area is compressive, and 78.5 kN at the negative loading respectively. The loading was controlled by the horizontal drift angle at a height corresponding to the second floor level (h: 615 mm). The loading was cyclic lateral loading at R = 1/1000 (1 cycle), 2/1000 (2 cycle), 5/1000, 7.5/1000, and 10/1000 (1 cycle respectively).

3.3 Test Results

The test results are listed in Table 3. In Table 3, the maximum strengths represent values at positive loadings. At the positive loadings of all specimens, the longitudinal reinforcement at the compressive end yielded at cycle R = 1/1000. At the final stage, all specimens crumbled and the strength decreased at the positive loadings. The load–deflection curves at the positive loadings are shown in Fig. 2. In the case of specimens with confining reinforcement, the limit drift angle of Specimens L3 and L4 which were confined at the corner and the area near the corner was larger than that of Specimen L2, which was confined at the corner only. The limit drift angle of Specimen L4, which had more confining reinforcement than Specimen L3, was larger than that of Specimen L3. These results show the effectiveness of concrete confinement. The drift angle of Specimen L1, which had no confining reinforcement, was larger than that of Specimen L2 which had confining reinforcement at the corner. The reason for these results is believed to be that the axial load of Specimen L1 was lower than that of the other specimens.

4. THE DEFORMATION CAPACITY OF CORE WALLS AND WALL COLUMNS BY CONFINING STEEL

In the lateral loading tests of core walls described in section 3, the failure mode of specimens was observed and the strain distribution of specimens was measured. From these test results, assumption for the formation of Eq. 2.1 fits the tests approximately. Therefore, the edge confinement index C_{ce} , which represents the deformation capacity of core walls and wall columns whose concrete is confined at the edge area, is proposed. In the index, the definition of depth-to-width ratio D/b in Eq. 2.1 is extended. Furthermore, the terms representing the confinement effect of the edge area concrete and confinement area by confining steel are added to Eq. 2.1.

4.1 Average Strain at Compressive End of Concrete Plastic Zone

Table 1 Physical Properties of Concrete

Specimen	Compressive Strength σ_B (N/mm ²)	Young's Modulus ($\times 10^4$ N/mm ²)	Split Strength (N/mm ²)
L1	52.6	2.97	3.74
L2	71.9	3.52	4.51
L3	70.9	3.40	4.82
L4	66.2	3.52	3.31

Table 2 Physical Properties of Steel

Bar Size	Yield Strength (N/mm ²)	Maximum Strength (N/mm ²)	Young's Modulus ($\times 10^5$ N/mm ²)	Elongation (%)
D10	360.7	518.9	1.85	18.2
D6	381.4	524.9	1.90	20.9
U5.1	1314.6	1397.5	1.91	7.5

Table 3 Test Results

Specimen	Maximum Strength		Limit Drift Angle ($\times 1/1000$ rad.)
	Exp.Load (kN)	Cal.Load (kN)	
L1	464	362	4.6
L2	377	440	3.1
L3	489	436	6.0
L4	557	417	9.6

Calculation⁷⁾

$$\mu_u = \{0.5 \cdot a_g \cdot \sigma_y \cdot g_1 \cdot D + 0.024 \cdot (1 + g_1) \cdot (3.6 - g_1) \cdot b \cdot D^2 \cdot F_c\} \cdot \{(N_{max} - N) / (N_{max} - N_b)\}$$

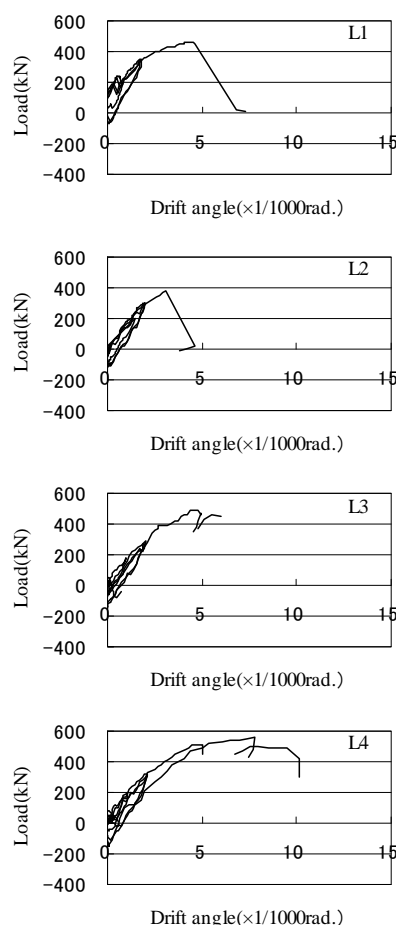


Fig. 2 Load – deflection curve

When applying Eq. 2.1 to the lateral loading tests of core walls described in section 3, σ_0/F_c and D/b are constant. From the distribution of vertical strain of confining steel and final failure mode of Specimens L2, L3 and L4, which were confined at the corner and the area near the corner, the concrete plastic zones of these specimens are considered to be identical. That is, index α representing the height of the concrete plastic zone of these specimens is considered to be identical. Therefore, among these specimens, the difference of drift angle R when the seismic capacity of wall columns begins to decrease is caused by the difference of ϵ_{cu} representing the average strain at the compressive end of the concrete plastic zone when the seismic capacity of wall columns begins to decrease. In the lateral loading tests of core walls, the confinement level of concrete and confinement area were the test parameters. Therefore, ϵ_{cu} differs among these specimens because of the differences in the amount of confining steel and confinement area.

On the other hand, the effect of confinement level of concrete and confinement area is considered to be included in ϵ_{cu} . That is, the effect of confinement level and confinement area on the drift angle R when the seismic capacity of wall columns begins to decrease, is not shown in a dependent form. Equation 2.1 is also intended for not 3-dimensional shear walls (core walls) but wall columns with rectangular section. Therefore, from the results of lateral loading tests of core walls described in section 3 and other tests of core walls and wall columns, the effect of confinement level of concrete, confinement area, and depth-to-width ratio on the drift angle R (the limit drift angle in this paper) when the seismic capacity of wall columns begins to decrease was examined as follows.

4.2 Confinement Area

Compressive strain at the bottom of the core wall Specimens 2, 3, and 4 was 1.0 – 2.5% at the final stage of lateral loading tests of core walls described in section 3. On the other hand, from the stress–strain curves obtained in the compressive tests which were conducted together with the lateral loading tests of core walls described in section 3, it was shown that the stress of specimens without confinement decreased suddenly when the strain exceeded 0.2%. Therefore, at the bottom of core walls, it is considered that the area without confinement cannot bear the compressive force at the strain of 1.0 – 2.5%. Near the final stage, the area where strain is less than 0.2% is small enough relative to the whole compressive area, and the stress at such area is small. Therefore, it is assumed that it is only the confined area, not the area without confinement, that bears the compressive force. The confinement area is shown in Fig. 3(a). Here, the ratio of the length of the confined concrete area in the horizontal wall length direction a to the compressive area length $(\sigma_0/F_c)D$, that is, $a/(\sigma_0/F_c)D$, is defined as the effective burden ratio of compressive force in the compressive area. $a/(\sigma_0/F_c)D$ is assumed to be a variable which influences ϵ_{cu} .

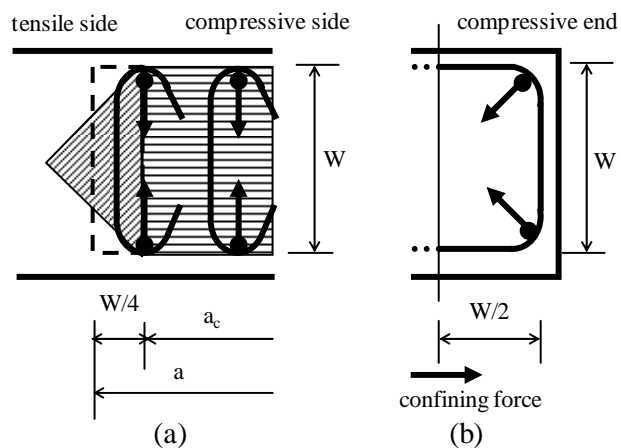


Fig. 3 Confinement area

In the definition of the length of the confined concrete area a , $W/4$ is added to the length of the confined core in the horizontal wall length direction a_c . Here, W is the minimum dimension of the confined core and is defined as the distance between the axes of confining steel. The reason for adding $W/4$ is the assumption that confining steel in the place furthest from the compressive end gives a confining effect to concrete without confinement. That is, the confining force is considered to act toward the center of the wall-thickness direction through the longitudinal reinforcement. In this

case, confining force is considered to be transmitted for compressive stress and the range of compressive stress spreads out as confining force is transmitted toward the center. According to observations of the fracture process in the above compression tests, fracture and exfoliation of concrete begin after maximum strength was reached. On the other hand, a certain part suffered no exfoliation even at the end of loading. The left part is considered to transmit compressive stress effectively to the end of loading. The range of this part was within 45 degrees from the central side of the wall-thickness direction. Therefore, the confining force is considered to be transmitted effectively within 45 degrees.

From the above findings, it is assumed that the confining force acts within 45 degrees and the transmission range is as shown by the angled-line area in Fig. 3(a). That is, it is assumed that the width of the confining core is W and the area of the triangle with angled lines is $W^2/4$. The triangle is replaced by a rectangle of equal area. The rectangle is enclosed by dashed lines in Fig. 3(a). The dimension of the rectangle in the wall length direction $W/4$ is added to the length of the confined core in the wall length direction a_c . On the other hand, the relationship of the confining reinforcement strain and the drift angle in the lateral loading tests of core walls described in section 3 showed that there was no confining force of confining steel in the tensile area of concrete. Therefore, it is assumed that the tensile area which includes the confining steel is not included in the confinement area. That is, in the case of $a/(\sigma_0/F_c)D > 1$, $a/(\sigma_0/F_c)D$ is 1.

4.3 Confinement Effect of Concrete

Like the results of the compression tests described above, the maximum strength and the stress after the maximum strength of confined concrete are larger than those of concrete which is not confined. These results are considered to depend on the confinement effect of confining steel. Regarding the confinement effect of concrete, Muguruma et al. proposed a lateral confinement index C_c . In this study, we used C_c as a variable to represent the confinement effect of concrete. C_c is defined as follows:

$$C_c = \rho_s \cdot f_y^{0.5} \cdot (1 - 0.5S/W)/f'_c \quad (4.1)$$

where ρ_s = volume ratio of confining steel; f_y = yield strength of confining steel; S = pitch of confining steel; W = minimum dimension of confining core section; f'_c = compressive strength of plain concrete. Figure 4 shows the relationship of the results of the compression tests described above and the strength calculated by applying C_c to the strength of a specimen without reinforcement in the compression tests. The figure shows that both of them match well. The authors also showed that Muguruma's equation with C_c closely matched the results of the compression tests of the square and rectangular section specimens in reference 4. In reference 4, Muguruma's equation also matched the test results at the stress descending area of the stress-strain curve.

The rectangular section specimens of the compression tests which were conducted together with the lateral loading tests of core walls described in section 3 had the confining reinforcement in the short-side direction, but no confining reinforcement in the long-side direction. In the case of the rectangular section, the fracture zone in the loading axis direction is considered to depend on the short-side direction more than on the long-side direction as shown in reference 2. That is, comparing the square section specimen and the rectangular section specimen whose short-side dimension was

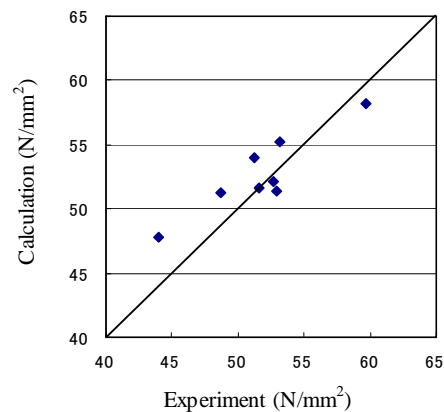


Fig. 4 Comparison of calculation and experiment

equal to one side of the square section specimen, the fracture zone in the loading axis direction of both specimens was about the same. The results of the compression tests related to the tests in section 3 were similar, too. Therefore, the maximum strength and the decreasing stress after the maximum strength of the compression tests are considered to depend on the confining in the short-side direction much more than in the long-side direction. From the above, it is considered that C_c can be applied to the confining effect of the panel concrete of core walls.

In the case that the shear reinforcement is the hoop type and surrounds the panel concrete, it was assumed that the shear reinforcement confines the edge area concrete as shown in Fig. 3(b). That is, the confining force was assumed to act toward the center of the wall-thickness direction and the wall length direction at 45 degrees through the corner longitudinal reinforcement. The confinement area of the shear reinforcement was assumed to be the dimension of $W/2$ from the end of the confinement area, and the volume of the reinforcement in this area was used to calculate volume ratio ρ_s in Eq. 4.1.

4.4 Depth-to-Width Ratio of 3-Dimensional Shear Walls

The depth-to-width ratio of wall columns is defined as D/b . On the other hand, that of 3-dimensional shear walls such as L-, T-, and H-shaped core walls is not defined. Therefore, the depth-to-width ratio of 3-dimensional shear walls was examined using the results of past studies as follows. The depth-to-width ratio of wall columns is defined as D/b . In this case, the depth of the wall column D is considered to be the distance between the compressive end and the tensile end in a horizontal section. Likewise, in the case of 3-dimensional shear walls, the distance between the compressive end and tensile end in the loading direction, that is, the length of

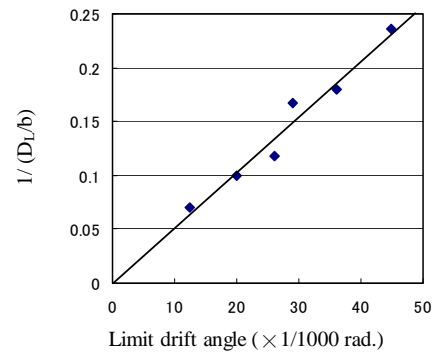


Fig. 5 Limit drift angle — $1/(D_L/b)$ relationship

the wall projected to the loading direction axis, is defined as the depth of the wall D_L . In references 8 and 9, lateral loading tests of L- and H-shaped 3-dimensional core walls were conducted respectively. The parameter of the tests was loading direction, and other conditions such as the properties of specimens and axial load were identical. From the load–deflection curves shown in reference 8 and 9, the relationship of the limit drift angle R_u and $1/(D_L/b)$ was examined. The limit drift angle R_u is defined as the drift angle when the load is less than 80% of the maximum load. Figure 5 shows the relationship of R_u and $1/(D_L/b)$ of both test series. This figure shows that $1/(D_L/b)$ is proportional to R_u . This relation is similar in the case of Eq. 2.1, which shows the drift angle when the seismic capacity of wall columns begins to decrease. That is, regarding the deformation capacity, D_L/b of 3-dimensional shear walls is similar to D/b of wall columns.

4.5 Edge Confinement Index

The relation of the parameters of average strain at the compressive end of the concrete plastic zone, confinement area, and confinement effect of concrete, is as follows.

$$\varepsilon_{cu} = \beta \cdot C_c \cdot \{a/(\sigma_0/F_c)D\} \quad (4.2)$$

where β = index. By multiplying both sides by α ,

$$\alpha \cdot \varepsilon_{cu} = \alpha \cdot \beta \cdot C_c \cdot \{a/(\sigma_0/F_c)D\} \quad (4.3)$$

Substituting Eqs. (4.3) and (4.4) for Eq. (2.1),

$$\alpha \cdot \beta = \gamma \quad (4.4)$$

$$R = \gamma \cdot Cc \cdot \{a/(\sigma_0/F_c)D\}/\{(\sigma_0/F_c) \cdot (D_L/b)\} \quad (4.5)$$

Substituting Eq. (4.6) for Eq. (4.5),

$$Cce = Cc \cdot \{a/(\sigma_0/F_c)D\}/\{(\sigma_0/F_c) \cdot (D_L/b)\} \quad (4.6)$$

$$R = \gamma \cdot Cce \quad (4.7)$$

Cce is defined as the edge confinement index, where Cc = lateral confinement index of Eq. (4.1); a = length of the confined concrete area in the horizontal wall length direction, in the case of $a/(\sigma_0/F_c)D > 1$, $a/(\sigma_0/F_c)D$ is 1, $a = a_c + W/4$; a_c = length of the confined core in the horizontal wall length direction; D = length of each side of core wall; b = thickness of core wall; D_L = length of core wall projected in loading direction axis.

Figure 6 shows the relationship between the edge confinement index Cce and limit drift angle Ru based on the results of lateral loading tests of core walls and wall columns conducted previously. The number of specimens was 52. Based on the descriptions of the references or the load-deflection curves shown in the references, the specimens were selected by confirming that the load decreased to less than 80% of the maximum load. When the axial load was different under positive loading and negative loading, the limit drift angle of the side where the axial load was larger was adopted. The compression area increases remarkably when the side of the transverse walls in T-shaped core walls, the side which was perpendicular to the loading direction of L-shaped core walls, and the flange in H-shaped core walls whose loading direction was the strong axis direction, are under compression. In such cases, the limit drift angle increases remarkably, so such cases were excluded here. When the transverse walls in T-shaped core walls and the webs in H-shaped core walls are under tension, their effect on the limit drift angle is very large. Therefore, the product of the yield strength of the longitudinal reinforcement and the total area of the longitudinal reinforcement was added to the axial load.

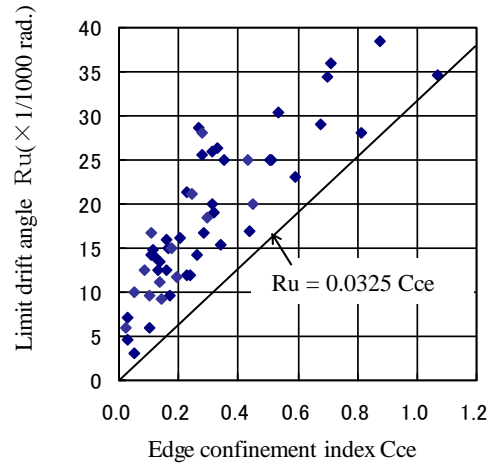


Fig. 6 Edge confinement index Cce
— limit drift angle Ru relationship

The selected specimens have concrete compressive strength values ranging from 21.9 to 134 N/mm², axial load ratio of 0.095 to 0.991, and depth-to-width ratio of 2.07 to 14.14. Figure 6 shows that the edge confinement index Cce and limit drift angle Ru are closely correlated. A straight line from the origin of the coordinates is found as the lower limit of Ru. By substituting the inclination of the line for γ , we obtain

$$\gamma = 0.0325 \quad (4.8)$$

The next equation is found as the lower limit calculated by Eq. (4.7):

$$Ru = 0.0325Cce \quad (4.9)$$

The limit drift angle of wall columns and core walls is found to be on the safe side by substituting the reinforcement arrangement of the edge area, the axial load, the shape of the cross section and so on in Eq. (4.9).

5. CONCLUSIONS

Based on the results of lateral loading tests of core walls and compression tests which simulated the corner area of core walls conducted previously by the authors and the results of previous studies on wall columns, the deformation capacity of core walls and wall columns was examined. The major findings were as follows:

- (1) The results of compression tests which simulated the corner area of core walls closely matched Muguruma's equation for the confinement effect of concrete.
- (2) Regarding the deformation capacity, the depth-to-width ratio of 3-dimensional shear walls is treated similarly to that of wall columns by defining the length of the wall projected to the loading direction axis as the depth of the wall.
- (3) The edge confinement index C_{ce} shown by Eq. (4.6) was proposed as an index for the deformation capacity of core walls and wall columns. When this index was applied to the results of lateral loading tests of core walls and wall columns, C_{ce} and limit drift angle R_u were closely correlated.
- (4) The limit drift angle of wall columns and core walls was found to be on the safe side by substituting the reinforcement arrangement of the edge area, the axial load, the shape of the cross section and so on in Eq. (4.9) in the range of conditions of selected specimens.

REFERENCES

- 1) Nakachi, T., Toda, T. and Tabata, K. (1996). Experimental Study on Deformation Capacity of Reinforced Concrete Core Walls After Flexural Yielding. *Proceedings of Eleventh World Conference on Earthquake Engineering*, Paper No. 1714.
- 2) Nakachi, T., Hiraishi, H. et al. (1986). Experimental Study on Effect of Partial Confinement on Broad Columns. *Summaries of Technical Papers of Annual Meeting of Architectural Institute of Japan*, 195–200.
- 3) Nakachi, T., Tsubosaki, H. et al. (1986). Effect of Confinement in Compressive Zone on Ductility of Columns with Large Depth-to-Width Ratio. *Proceedings of Seventh Japan Earthquake Engineering Symposium*, 1189–1194.
- 4) Muguruma, H. et al. (1983). Study on Improving the Ductility of High Strength Concrete by Lateral Confining: Part 2. Modeling of Stress-Strain Relations. *Summaries of Technical Papers of Annual Meeting of Architectural Institute of Japan*, 1915–1916.
- 5) Nakachi, T., Hiraishi, H. et al. (1987). Experimental Study on Deformation Capacity of Wall Columns. *Summaries of Technical Papers of Annual Meeting of Architectural Institute of Japan*, 191–196.
- 6) Hiraishi, H., Inai, E. et al. (1992). Evaluation of Seismic Capacity of Wall Columns in High-Rise Reinforcement Concrete Frame Structures. *Journal of Structural and Construction Engineering (Transactions of AIJ)*, **528**, 133–144.
- 7) AIJ. (1990). Ultimate Strength and Deformation Capacity of Buildings in Seismic Design, Gihodo Shuppan.
- 8) Takeda, C., Arai, Y., Mizoguchi, M. (1994). Bending Ultimate Strength of RC L-shaped Section Wall Subjected to Bi-directional Horizontal Forces and Normal Force. *Summaries of Technical Papers of Annual Meeting of Architectural Institute of Japan*, 293–294.
- 9) Bessho, S., Maruta, M., et al. (1997). Experimental Study on H-shape Type RC Core-Wall. *Summaries of Technical Papers of Annual Meeting of Architectural Institute of Japan*, 185–188.